

Supporting Information for

Metabolic Approaches to Understanding Climate Change Impacts on Seasonal Host-Macroparasite Dynamics

Péter K. Molnár, Susan J. Kutz, Bryanne M. Hoar, Andrew P. Dobson

CONTENT:

Figure S1 Sensitivity of development time ($\tau_L(T)$), mortality rate ($\mu_L(T)$), and $R_0(T)$, to the parameters of equation 3 (pp. 2-4)

Figure S2 Model predictions for impacts of climate change on seasonal parasite R_0 under the high uptake scenario (p. 5).

Appendix S1 Implications of a temperature-dependent parasite uptake rate, with Figures S3-S5 (p. 6-11)

Figure S3 Rates of parasite uptake, $\rho(T)H$, and the resultant $R_0(T)/C$ for the temperature-dependent uptake rate case (p. 9)

Figure S4 Model predictions for climatic impacts on seasonal parasite R_0 when parasite uptake rate by hosts is temperature-dependent, and mean annual temperature is varied (p. 10).

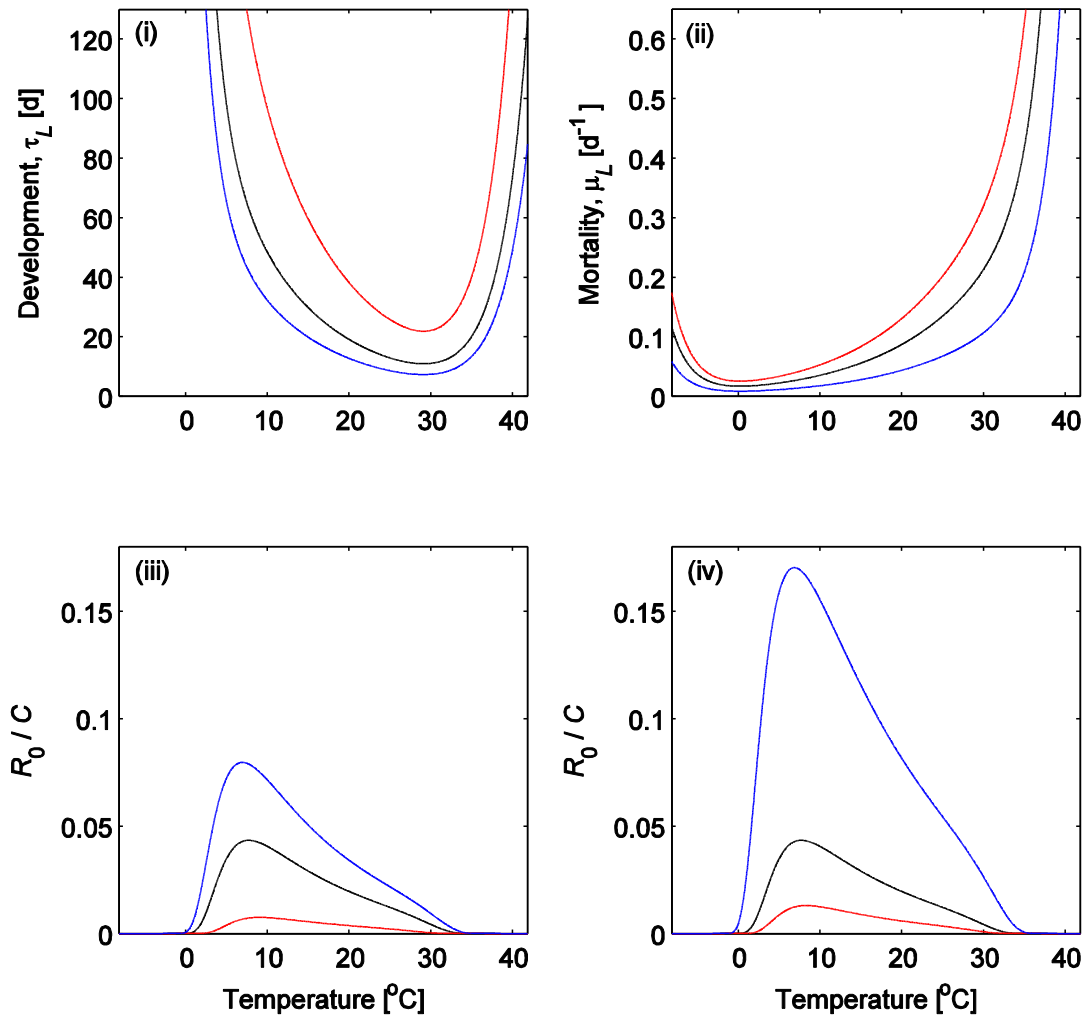
Figure S5 Model predictions for climatic impacts on seasonal parasite R_0 when parasite uptake rate by hosts is temperature-dependent, and the annual temperature amplitude is varied (p. 11).

Table S1 Data sources for the estimated activation energies of free-living parasitic nematode larvae, shown in Figure 5 of the main text (p. 12).

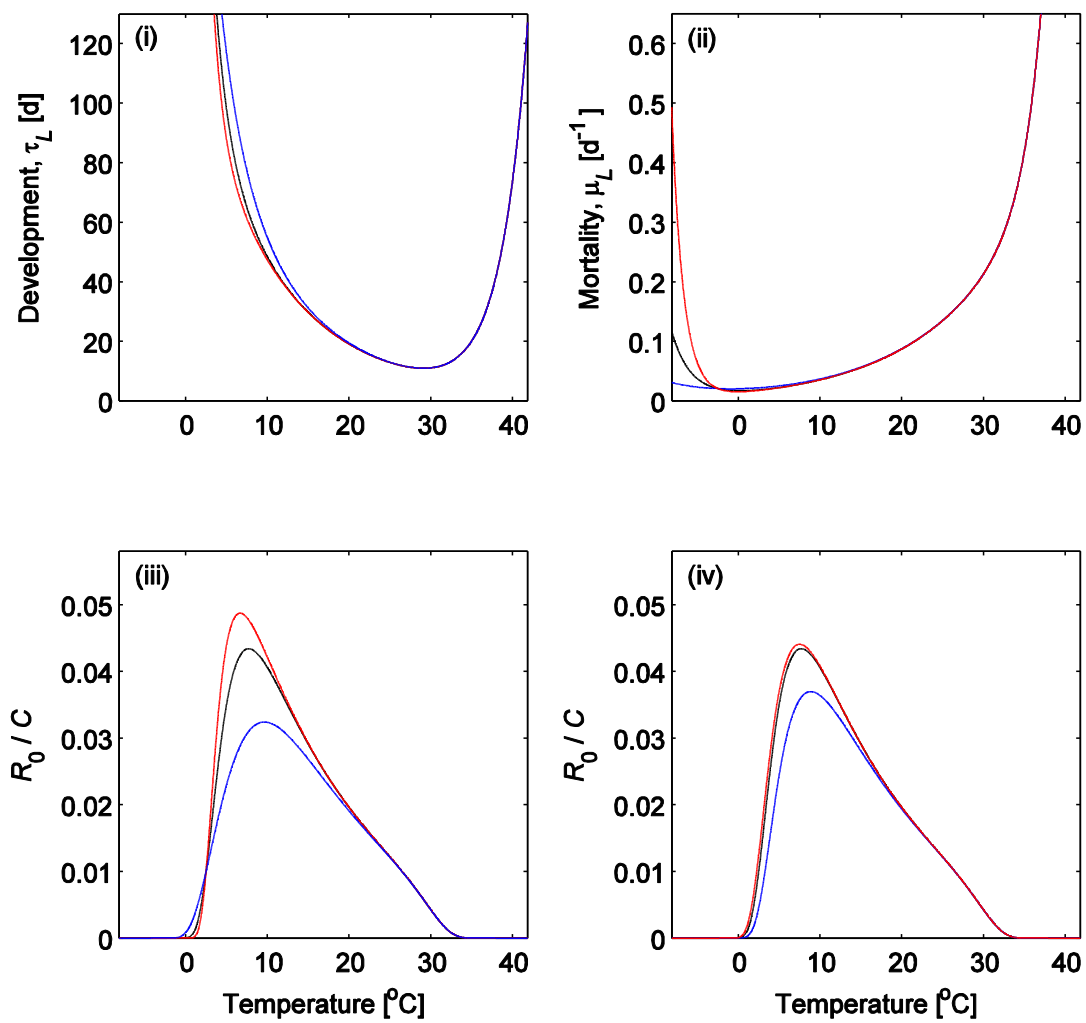
References for Supporting Information (p. 13-14).

Figure S1 Sensitivity of development time ($\tau_L(T)$), mortality rate ($\mu_L(T)$), and $R_0(T)$, to the parameters of equation 3. Left columns in (a-c) show the effect of parameter changes in the Sharpe-Schoolfield model of development (equation 3a), while holding the parameters of our analogous model of mortality (equation 3b) at their baseline values; right columns show the reverse case. In each panel, the first row shows how parameter changes affect $\tau_L(T)$ and $\mu_L(T)$, whereas the second row shows how these changes translate to changes in $R_0(T)$, calibrated to the scaling constant C (cf. equation 5). Effects are shown for decreasing (blue lines) or increasing (red lines) (a) the average development time (τ_0) and larval mortality (μ_0) at T_0 , (b) the low temperature inactivation energies E_τ^L and E_μ^L , and (c) the high temperature inactivation energies E_τ^H and E_μ^H from their baseline values (black lines). All baseline parameters and boundaries for the sensitivity analyses are shown in Table 2. All panels are based on the low uptake scenario, $\rho H = 0.01 \text{ d}^{-1}$.

(a)



(b)



(c)

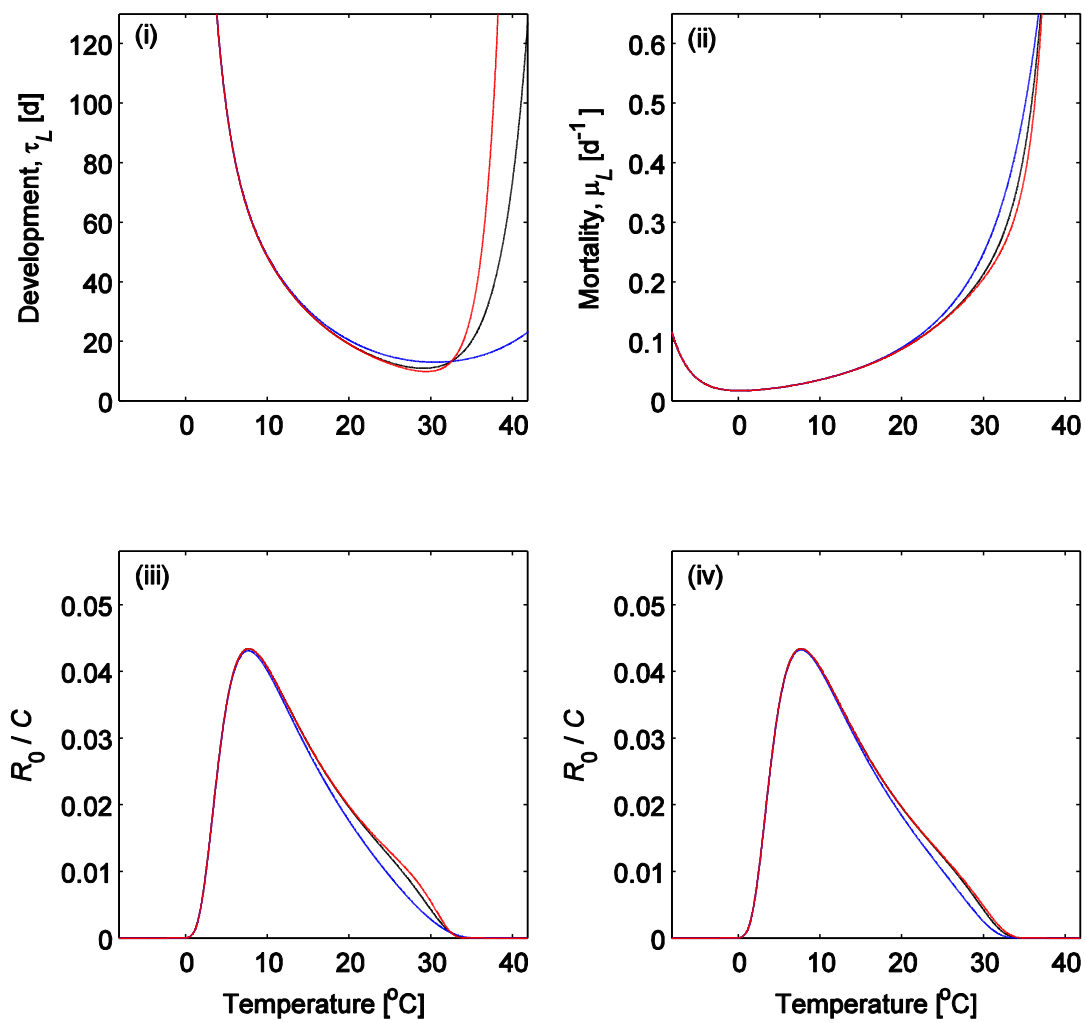
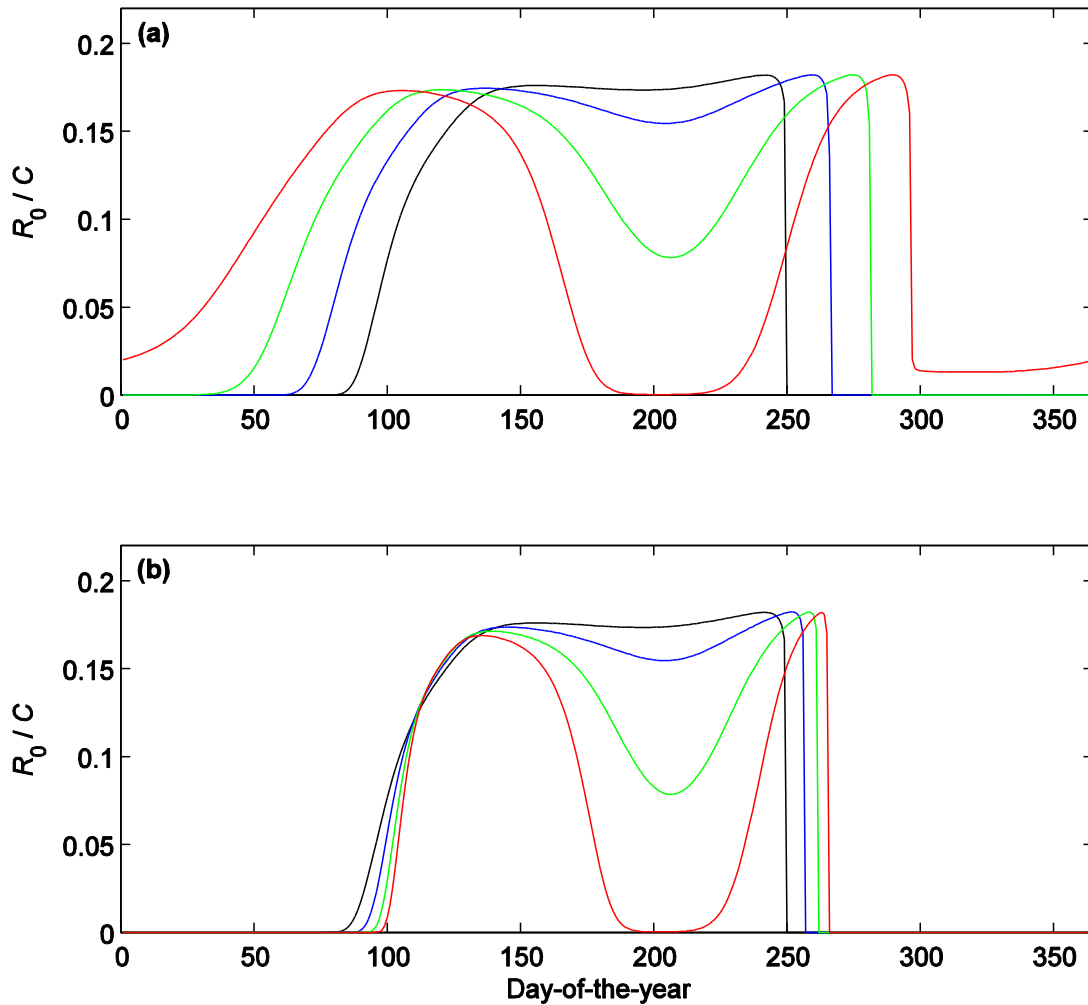


Figure S2 Model predictions for climate change impacts on seasonal parasite R_0 under the high uptake scenario. Expected lifetime reproductive output, R_0 (calibrated to the scaling constant $C=\lambda D_p/(\alpha_H+b_H+\mu_p)$), as a function of parasite birth date for parasite populations experiencing high uptake ($\rho H=1 \text{ d}^{-1}$). Results are based on the Sharpe-Schoolfield model for development, our analogous model of mortality (equation 3), and the seasonal host-parasite model (equations 6-9). Parameter estimates for development and mortality are the same as for the low uptake case (Fig. 4b-d, g-i). (a) Climate scenarios, specified by equation 6, with annual temperature amplitude held constant ($d_K = 20^\circ\text{C}$) and mean annual temperatures varied: $c_K = 0^\circ\text{C}$ (black lines), 5°C (blue lines), 10°C (green lines), and 15°C (red lines). (b) Climate scenarios with mean annual temperature held constant ($c_K = 0^\circ\text{C}$) and temperature amplitude varied: $d_K = 20^\circ\text{C}$ (black lines), 25°C (blue lines), 30°C (green lines), and 35°C (red lines).



Appendix S1. Implications of a Temperature-Dependent Parasite Uptake Rate.

The rate of parasite uptake by hosts, $\rho(T)H$, is determined by the encounter rate between hosts and patches that contain free-living larvae, and the encounter rate between hosts and larvae when hosts forage within such patches (Cornell *et al.* 2004). The former of these two factors will be determined by the movement patterns and speed of hosts, as well as the distribution of larval patches. Patch distribution, in turn, will also be determined by host movement (e.g., through the locations of fecal deposits), but will not be influenced significantly by active parasite movement as larval speed is usually orders of magnitude smaller than host speed. Because host movement can be assumed temperature-independent for endotherms, we consider the encounter rate between hosts and larval patches as roughly temperature-independent.

The second component of parasite uptake (encounter rate between hosts and larvae within patches), by contrast, may be influenced substantially by larval movement patterns and speed, and thus potentially temperature. Consider, for example, newly shed parasite larvae that are deposited within host feces. Often hosts will actively avoid such fecal pats when foraging (e.g., van der Wal *et al.* 2000), so that the encounter rate between larvae and hosts would increase with larval movement out of, and away from, these pats (Stromberg 1997). The exact influence of temperature is, however, difficult to determine. In some cases, larvae may disperse passively (e.g., through the influence of abiotic factors, such as wind or rain) but are otherwise immobile (e.g., *Ascaris spp.* where larvae develop within the egg). In these cases, it is reasonable to assume that parasite uptake rate is temperature-independent. In other species, larvae may move actively (Saunders *et al.* 2000; van Dijk & Morgan 2011), and larval speed, v_L , could be assumed to scale with the Boltzmann factor (Brown *et al.* 2004) or a temperature-dependent unimodal model (Dell *et al.* 2011). The rate at which larvae move away from the center of fecal pats, and thus the encounter rate with hosts, could then scale with v_L (if larvae move in relatively straight lines), the square root of v_L (if larval motion is described by an uncorrelated random walk), or more complicated functions that depend on the precise mechanisms of dispersal (e.g., *Dictyocaulus viviparus* where larvae initially disperse from fecal pats using exploding fungal spores as vehicles). Further complications may arise if larvae migrate from the soil surface to the tip of grass blades once outside the fecal pat to increase their probability of being ingested (Silangwa & Todd 1964). Notwithstanding potential influences of other environmental covariates, such as moisture or daylight, this process again may or may not be temperature-dependent (Saunders *et al.* 2000), possibly scaling host-larvae encounter rate with the Boltzmann factor, a unimodal model, or even a temperature-dependent step function if the decision to migrate upwards depends on temperature surpassing a certain threshold.

Few data exist to determine the precise role of temperature on uptake rate in most species, and a clear temperature dependence of this rate is often difficult to demonstrate empirically in field studies even in species with relatively mobile larvae, such as *Ostertagia ostertagi* (Grenfell *et al.* 1986). Nevertheless, we here use the simple case of describing $\rho(T)H$ through the Van't Hoff-Arrhenius relation

$$(S1a) \quad \rho(T) \cdot H = \rho_0 H e^{-\frac{E_\rho}{k} \left(\frac{1}{T} - \frac{1}{T_0} \right)}$$

or the Sharpe-Schoolfield model

$$(S1b) \quad \rho(T) \cdot H = \rho_0 H e^{-\frac{E_\rho}{k} \left(\frac{1}{T} - \frac{1}{T_0} \right)} \cdot \left(1 + e^{\frac{E_\rho^L}{k} \left(\frac{1}{T} - \frac{1}{T_\rho^L} \right)} + e^{\frac{E_\rho^H}{k} \left(-\frac{1}{T} + \frac{1}{T_\rho^H} \right)} \right)^{-1}$$

to show that inclusion of temperature-dependence in $\rho(T)H$ is unlikely to alter the qualitative conclusions, and will only marginally affect the quantitative conclusions, that were derived in the main text for R_0 for the temperature-independent case $\rho(T)H \equiv \rho_0 H$. For comparability with the temperature-independent case, we again consider low and high uptake scenarios, setting $\rho_0 H = 0.01 \text{ d}^{-1}$ and $\rho_0 H = 1 \text{ d}^{-1}$, respectively, and using the reference temperature $T_0 = 15^\circ\text{C}$. Further, we set the activation energy $E_\rho = 0.65 \text{ eV}$, and explore potential sensitivities to this parameter by varying it between 0.2 eV and 1.2 eV. The inactivation energies and threshold temperatures were set $E_\rho^L = E_\rho^H = 3.25 \text{ eV}$, $T_\rho^L = 2.5^\circ\text{C}$ and $T_\rho^H = 32.5^\circ\text{C}$, in analogy to the parameter values used for development.

As for the case with temperature-independent uptake ($\rho(T)H \equiv \rho_0 H$), R_0 is unimodal as a function of temperature. Hereby, $R_0(T)$ remains right-skewed when $\rho(T)$ is relatively insensitive to temperature ($E_\rho = 0.2 \text{ eV}$), but levels out ($E_\rho = 0.65 \text{ eV}$) and eventually becomes left-skewed ($E_\rho = 1.2 \text{ eV}$) with increasing temperature sensitivity (Fig. S3). This change in skewness is a direct consequence of the positive relation between temperature and $\rho(T)$ over most of the biologically relevant temperature range, because this implies increased parasite uptake, and thus increased $R_0(T)$, at high temperatures (and vice versa at low temperatures; Fig S3a). While these differences to the temperature-independent uptake case are pronounced for the low uptake scenario (Fig. S3a,b), the temperature-dependence of $\rho(T)$ plays a negligible role in the high uptake scenario as the proportion of larvae that enter a host (represented by $\rho(T)H / (\mu_L(T) + \rho(T)H)$ in equation 5) is already near unity for most of the temperature range (Figs. S3c,d). All of these results are independent of whether $\rho(T)$ is represented by the Van't Hoff-Arrhenius relation (equation S1a) or the Sharpe-Schoolfield model (equation S1b); both models yield nearly indistinguishable curves for $R_0(T)$, because equations S1a and S1b do not differ substantially at intermediate temperatures and because $R_0(T)$ is primarily determined by the limitations of development and mortality, rather than the limitations of uptake, at the temperature extremes.

Despite the differing temperature-dependencies of $R_0(T)$ for the temperature-independent and temperature-dependent uptake rate cases, model predictions are largely similar for the two cases when seasonality is incorporated. All conclusions regarding the general shape of the seasonally dependent R_0 , the impacts of climate change, and, in particular, the phenological shifts of the transmission pulses remain qualitatively unaltered both for climate scenarios with changing temperature means (Fig. S4) and for scenarios with changing temperature amplitudes (Fig. S5). A summer trough, for example, is

predicted for both the temperature-dependent and temperature-independent uptake cases, as this pattern is driven by the seasonality of development and mortality (cf. Figs. 4d,i in main text). The most marked difference between the two cases concerns the magnitude of the spring and fall R_0 -peaks, which are approximately equal with temperature-dependent parasite uptake, even in the low uptake scenario (Figs. S4b,e, S5b,e). This is because the rate of parasite uptake generally increases with increasing temperatures (Figs. S4a,d, S5a,d), conferring an advantage to spring-born larvae over larvae born in fall, thereby leveling out the uneven peaks of the temperature-independent uptake case (compare Figs. S4b,c, S5b,c). For the same reason, the expected summer troughs are slightly less pronounced in the temperature-dependent uptake case than in the temperature-independent uptake case. In the high uptake scenario, the temperature-dependence of uptake is negligible (Figs. S4d-f, S5d-f) for analogous reasons as outlined above for Fig. S3.

Figure S3. Rates of parasite uptake, $\rho(T)H$, and the resultant $R_0(T)/C$ as a function of temperature for the (a, b) low and (c, d) high uptake scenarios, respectively. Results are shown for three different activation energies (blue lines: $E_p=0.2$ eV; thin black lines: $E_p=0.65$ eV; red lines: $E_p=1.2$ eV). The results for the temperature-independent uptake case ($\rho(T)H \equiv 0.01$ d⁻¹ and $\rho(T)H \equiv 1$ d⁻¹, respectively) are re-plotted from Fig. 2 (main text) for comparison (thick black lines). Results are based on the unimodal models for development (equation 3a), mortality (equation 3b), and uptake rate (equation S1b); using the Van't Hoff-Arrhenius relation for uptake rate (equation S1a) instead, yields nearly indistinguishable results for $R_0(T)/C$ as plotted here, so this case is not shown explicitly.

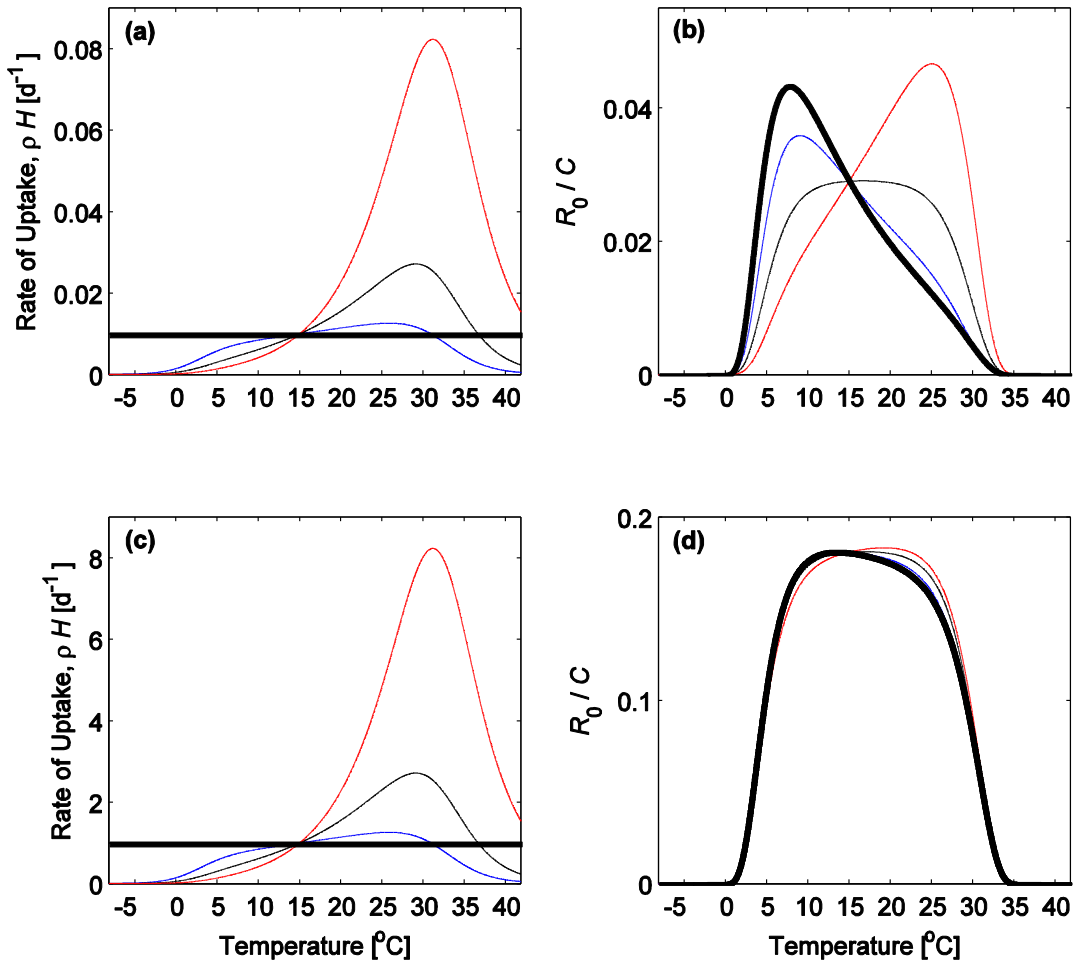


Figure S4 Model predictions for climatic impacts on seasonal parasite R_0 when parasite uptake rate by hosts is temperature-dependent, and mean annual temperature is varied. (a) Day-of-the-year-specific rate of parasite uptake by hosts, $\rho(T)H$, and (b) the resultant R_0/C as a function of parasite birth date for the low uptake scenario. Results are based on the unimodal models for development (equation 3a), mortality (equation 3b), and uptake rate (equation S1b). (c) is re-plotted from Fig. 4e (main text) to facilitate comparison, and shows the birth date-dependent R_0/C when uptake rate is temperature-independent, i.e., when $\rho(T)H \equiv 0.01 \text{ d}^{-1}$ for all temperatures. Climate scenarios are as in Figs. 4a-e and S2a, with annual temperature amplitude held constant ($d_K = 20^\circ\text{C}$) and mean annual temperatures varied: $c_K = 0^\circ\text{C}$ (black lines), 5°C (blue lines), 10°C (green lines), and 15°C (red lines). (d-f) are as (a-c) but for the high uptake scenario (panel (f) is Fig. S2a re-plotted to facilitate comparison).

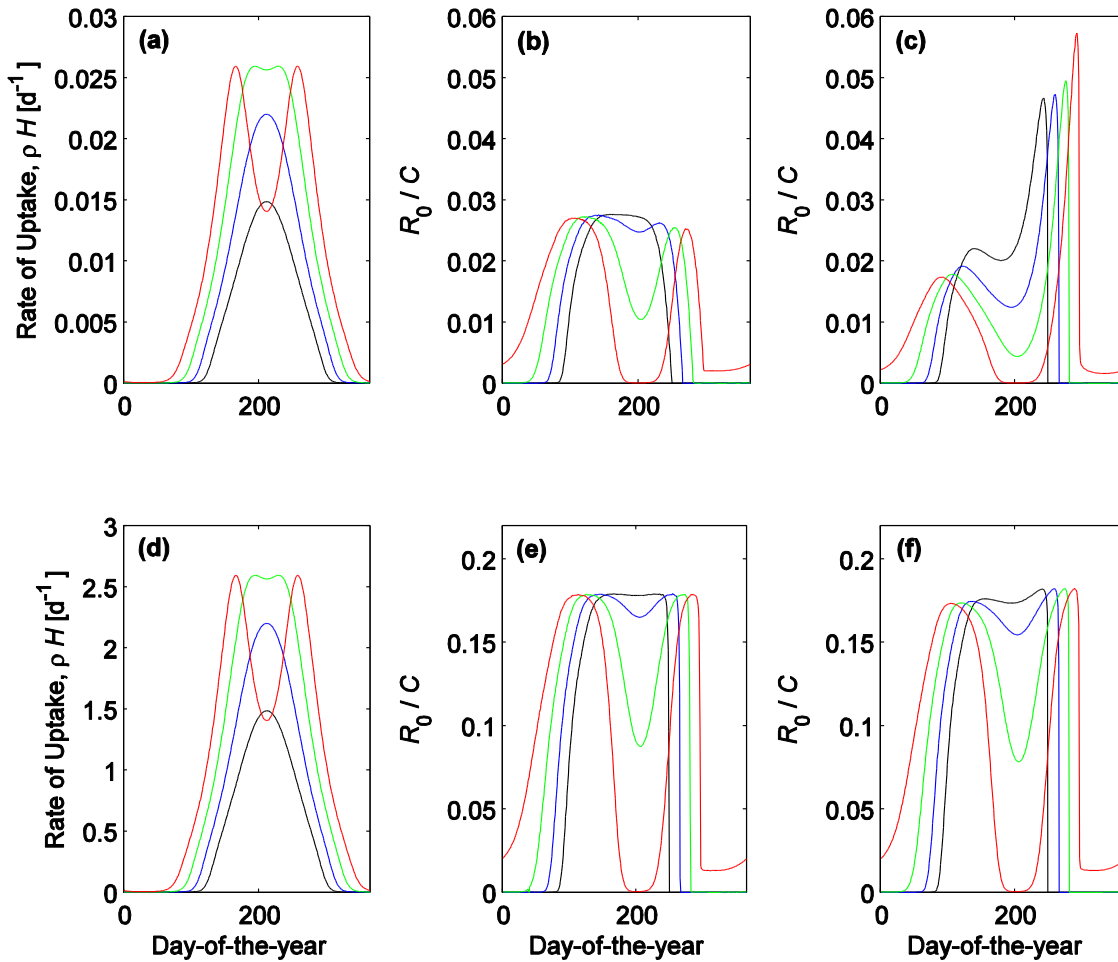


Figure S5 Model predictions for climatic impacts on seasonal parasite R_0 when parasite uptake rate by hosts is temperature-dependent, and the annual temperature amplitude is varied. (a) Day-of-the-year-specific rate of parasite uptake by hosts, $\rho(T)H$, and (b) the resultant R_0/C as a function of parasite birth date for the low uptake scenario. Results are based on the unimodal models for development (equation 3a), mortality (equation 3b), and uptake rate (equation S1b). (c) is re-plotted from Fig. 4j (main text) to facilitate comparison, and shows the birth date-dependent R_0/C when uptake rate is temperature-independent, i.e., when $\rho(T)H \equiv 0.01 \text{ d}^{-1}$ for all temperatures. Climate scenarios are as in Figs. 4f-j and S2b, with mean annual temperature held constant ($c_k = 0^\circ\text{C}$) and temperature amplitude varied: $d_k = 20^\circ\text{C}$ (black lines), 25°C (blue lines), 30°C (green lines), and 35°C (red lines). (d-f) are as (a-c) but for the high uptake scenario (panel (f) is Fig. S2b re-plotted to facilitate comparison).

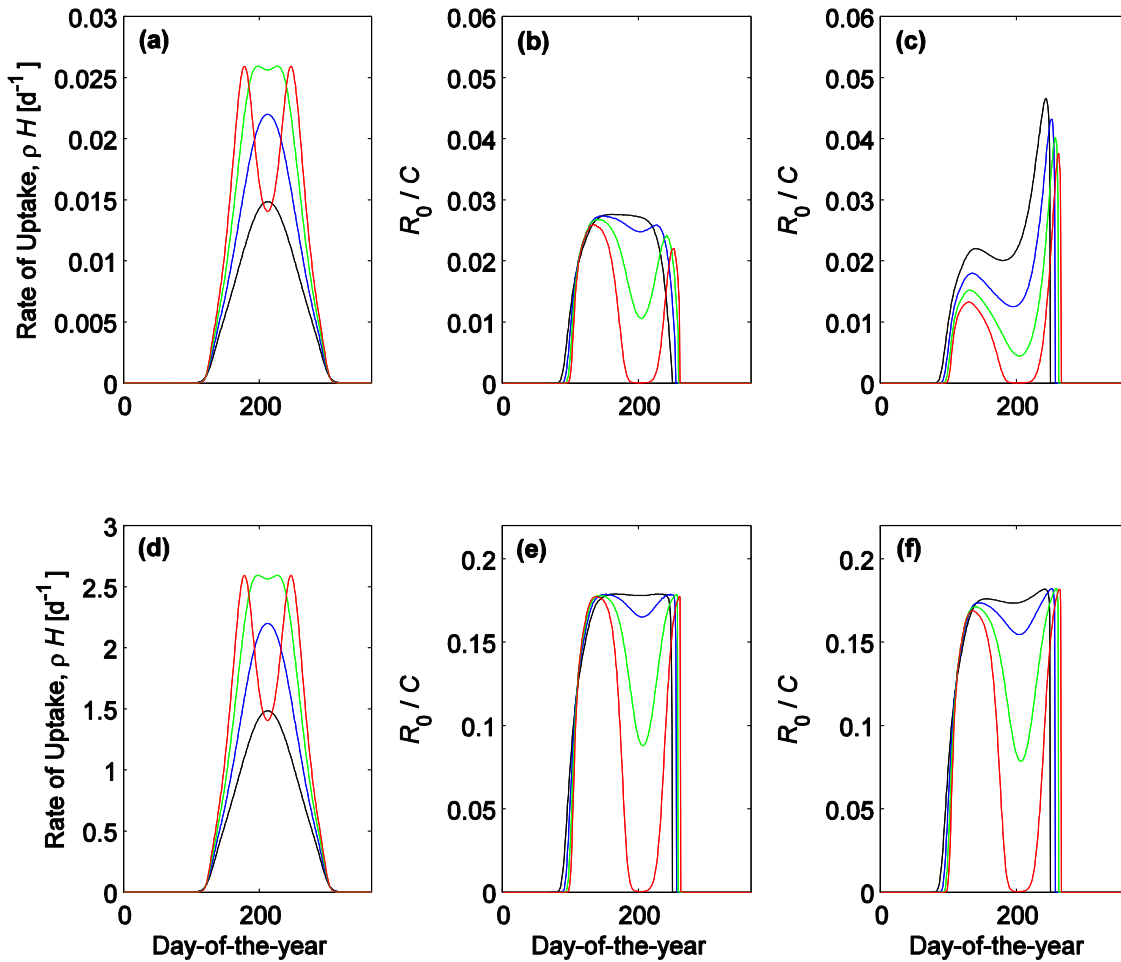


Table S1 Data sources for the estimated activation energies of free-living parasitic nematode larvae, shown in Figure 5 (main text). Activation energies were estimated by fitting equations 2a and 2b (main text) to the temperature-dependent development and mortality data reported in these studies. We used the full temperature range of each source study for model fitting, except where the data suggested threshold effects that could only be captured by the Sharpe-Schoolfield model. In these cases (development: *O. ostertagia*, $T \leq 5^{\circ}\text{C}$, *H. contortus*, $T \leq 17.8^{\circ}\text{C}$, $T \geq 34.4^{\circ}\text{C}$; mortality: *Nematodirus* spp., $T \geq 30^{\circ}\text{C}$), we excluded these temperature extremes and used the remaining data for fitting. In species with more than one dataset, we averaged estimated activation energies to avoid pseudoreplication.

Species	Source
Development	
<i>Nematodirus battus</i>	van Dijk & Morgan 2008
<i>Trichostrongylus vitrinus</i>	Beverigde <i>et al.</i> 1989
<i>Haemonchus contortus</i>	Berberian & Mizelle 1957
<i>Teladorsagia circumcincta</i>	Gibson 1981; Salih & Grainger 1982
<i>Ostertagia ostertagi</i>	Young <i>et al.</i> 1980
<i>Ostertagia gruehneri</i>	This study
Mortality	
<i>Dictyocaulus filaria</i>	Boag & Thomas 1985
<i>Nematodirus spathiger</i>	Boag & Thomas 1985
<i>Nematodirus filicollis</i>	Boag & Thomas 1985
<i>Nematodirus battus</i>	Boag & Thomas 1985
<i>Trichostrongylus axei</i>	Boag & Thomas 1985
<i>Trichostrongylus colubriformis</i>	Boag & Thomas 1985
<i>Trichostrongylus retortaeformis</i>	Boag & Thomas 1985
<i>Cooperia curticei</i>	Boag & Thomas 1985
<i>Cooperia oncophora</i>	Boag & Thomas 1985
<i>Haemonchus contortus</i>	Boag & Thomas 1985
<i>Teladorsagia circumcincta</i>	Boag & Thomas 1985
<i>Ostertagia ostertagi</i>	Boag & Thomas 1985
<i>Ostertagia gruehneri</i>	This study

References for Supporting Information

- Berberian, J.F. & Mizelle, J.D. (1957). Developmental studies on *Haemonchus contortus* Rudolphi (1803). *Am. Midl. Nat.*, 57, 421-439.
- Beveridge, I., Pullman, A.L., Martin, R.R. & Barelds, A. (1989). Effects of temperature and relative humidity on development and survival of the free-living stages of *Trichostrongylus colubriformis*, *T. rugatus* and *T. vitrines*. *Vet. Parasitol.*, 33, 143-153.
- Boag B. & Thomas, R.J. (1985). The effect of temperature on the survival of infective larvae of nematodes. *J. Parasitol.*, 71, 383-384.
- Brown, J.H., Gillooly, J.F., Allen, A.P., Savage, V.M. & West, G.B. (2004). Toward a metabolic theory of ecology. *Ecology*, 85, 1771-1789.
- Cornell, S.J., Isham, V.S. & Grenfell, B.T. (2004). Stochastic and spatial dynamics of nematode parasites in farmed ruminants. *Proc. R. Soc. B*, 271, 1243-1250.
- Dell, A.I., Pawar, S. & Savage, V.M. (2011). Systematic variation in the temperature dependence of physiological and ecological traits. *Proc. Nat. Acad. Sci.*, 108, 10591-10596.
- Gibson, M. (1981). The effect of constant and changing temperatures on the development rates of the eggs and larvae of *Ostertagia ostertagi*. *J. Therm. Biol.*, 6, 389-394.
- Grenfell, B.T., Smith, G. & Anderson, R.M. (1986). Maximum-likelihood estimates of the mortality and migration rates of the infective larvae of *Ostertagia ostertagi* and *Cooperia oncophora*. *Parasitology*, 92, 643-652.
- Salih, N.E. & Grainger, J.N.R. (1982). The effect of constant and changing temperatures on the development of the eggs and larvae of *Ostertagia circumcincta*. *J. Therm. Biol.*, 7, 35-38.
- Saunders, L.M., Tompkins, D.M. & Hudson, P.J. (2000). Spatial aggregation and temporal migration of free-living stages of the parasitic nematode *Trichostrongylus tenuis*. *Funct. Ecol.*, 14, 468-473.
- Silangwa, S.M. & Todd, A.C. (1964). Vertical migration of trichostrongylid larvae on grasses. *J. Parasitol.*, 50, 278-285.
- Stromberg, B.E. (1997). Environmental factors influencing transmission. *Vet. Parasitol.*, 72, 247-264.
- van der Wal, R., Irvine, J., Stien, A., Shepherd, N. & Albon, S.D. (2000). Faecal avoidance and the risk of infection by nematodes in a natural population of reindeer. *Oecologia*, 124, 19-25.

- van Dijk J. & Morgan, E.R. (2008). The influence of temperature on the development, hatching and survival of *Nematodirus battus* larvae. *Parasitology*, 135, 269-283.
- van Dijk, J. & Morgan, E.R. (2011). The influence of water on the migration of infective trichostrongyloid larvae onto grass. *Parasitology*, 138, 780-788.
- Young, R.R., Nicholson, R.M., Tweedie, R.L. & Schuh, H.J. (1980). Quantitative modelling and prediction of development times of the free-living stages of *Ostertagia ostertagi* under controlled and field conditions. *Parasitology*, 81, 493-505.